Magnetically Induced Current Densities in Aromatic, Antiaromatic, Homoaromatic, and Nonaromatic Hydrocarbons

Heike Fliegl

Institut für Nanotechnologie, Forschungszentrum Karlsruhe GmbH, Hermann-von-Helmholtz-Platz 1, D-76344 Eggenstein-Leopoldshafen, Germany

Dage Sundholm*

Department of Chemistry, P.O. Box 55 (A.I. Virtanens plats 1), FIN-00014 University of Helsinki, Finland

Stefan Taubert

Department of Chemistry, P.O. Box 55 (A.I. Virtanens plats 1), FIN-00014 University of Helsinki, Finland

Jonas Jusélius

Department of Chemistry, University of Tromsø, N-9037 Tromsø, Norway

Wim Klopper

Institut für Physikalische Chemie, Universität Karlsruhe (TH), Engesser Str. 15, D-76131 Karlsruhe, Germany

Received: April 1, 2009; Revised Manuscript Received: June 5, 2009

The magnetically induced current densities for ring-shaped hydrocarbons are studied at the density functional theory (DFT) and second-order Møller−Plesset (MP2) levels using gauge-including atomic orbitals. The current densities are calculated using the gauge-including magnetically induced current approach. The calculations show that all studied hydrocarbon rings sustain strong diatropic and paratropic ring currents when exposed to an external magnetic field, regardless whether they are unsaturated or not. For nonaromatic rings, the strength of the paratropic current flowing inside the ring is as large as the diatropic one circling outside it, yielding a vanishing net ring current. For aromatic molecules, the diatropic current on the outside of the ring is much stronger than the paratropic one inside, giving rise to the net diatropic ring current that is typical for aromatic molecules. For antiaromatic molecules, the paratropic ring-current contribution inside the ring dominates. For homoaromatic molecules, the diatropic current circles at the periphery of the ring. The ring current is split at the CH_2 moiety; the main fraction of the current flow passes outside the CH_2 at the hydrogens, and some current flows inside the carbon atom. The diatropic current does not take the through-space short-cut pathway, whereas the paratropic current does take that route. Calculations of the ring-current profile show that the ring current of benzene is not transported by the π electrons on both sides of the molecular ring. The strongest diatropic ring current flows on the outside of the ring and in the ring plane. A weaker paratropic current circles inside the ring with the largest current density in the ring plane. Due to the ring strain, small unconjugated and saturated hydrocarbon rings sustain a strong ring current which could be called ring-strain current. Nuclear magnetic shieldings calculated for 1,3,5-cycloheptatriene and homotropylium at the DFT and MP2 levels agree well with experimental values.

I. Introduction

The strength and pathway of the magnetically induced current flow sustained by delocalized electrons in molecular systems might play an important role in nanotechnological applications. For example, metamaterials consisting of split nanosized gold rings have been found to have unusual magnetic response properties yielding a negative index of refraction for wavelengths in the micrometer region.[1−3] As the resonance wavelength scales linearly with the size of the circuit, a resonator in the visible range must be at least a factor of 3 smaller. Ring-shaped, electron-rich hydrocarbons with a slit cutting the delocalization pathway might be a good starting point for the design of carbon-

based resonant circuits (LC circuits) with a resonance frequency in the visible region. However, the realization of carbon-based LC circuits can encounter difficulties because hydrocarbons rings with a slit are known to sustain ring currents, even though the molecular conjugation is interrupted by single bonds. That class of molecules is called homoaromatic molecules.[4−19] The homoaromaticity concept introduced in the 1960s has awakened interest in the aromaticity renaissance of the 21st century.[6,20−27] Molecular aromaticity has also been suggested to be multidimensional because employed criteria yield in some cases different degrees of aromaticity.[28−33] Recent studies of the aromaticity of polycyclic aromatic (PAH)[34,35] and antiaromatic (PAAH)[36] hydrocarbons indicate that there is no need to introduce a multidimensional aromaticity character for these classes of molecules. For more complex aromatic molecules,

* Corresponding author E-mail: Dage.Sundholm@helsinki.fi.

the disagreement between the obtained degrees of aromaticity might be due to inaccuracies in the employed methods to assess the aromaticity or due to the interpretation of the results. Novel computational tools such as the gauge-including magnetically induced current (GIMIC) method render unambiguous calculations of the magnetically induced current strengths and current pathways feasible.[37] Here, we use gimic to calculate the magnetically induced ring-current strengths and to assess the degree of molecular aromaticity and electron delocalization. The strength of the ring current circling around molecular rings has been proven to be an accurate and reliable method to rank the molecular aromaticity.[37-40] The current pathways and the flow along chemical bonds and around molecular rings reflect the electron delocalization in metal clusters[41,42] and yield aromaticity properties of complex multiring molecules such as porphyrins, fullerenes, and hydrocarbon nanorings.[35-37,43-45]

In this study, the magnetically induced current densities are calculated for aromatic, antiaromatic, homoaromatic, and nonaromatic hydrocarbon rings to provide novel insights into the current transport in molecules with a slit cutting the electron delocalization pathway. As an example of aromatic molecules, the current density of benzene is investigated. Cyclobutadiene is chosen to represent antiaromatic molecules. The archetypal homoaromatic molecule is the homotropylium (homotropenylium) cation ($C_8H_9^+$) consisting of a tropylium ($C_7H_7^+$) ring fused with a CH_2 moiety.[46,47] The aromaticity of homotropylium is experimentally observed by measuring the ^1H NMR chemical shifts of the CH_2 hydrogens.[46,47] Other potentially homoaromatic molecules can be derived from cyclic and conjugated hydrocarbons, fulfilling Hückel's $(4n + 2)$ π-electron rule, by fusing a CH_2 unit into a C—C bond of the molecular ring. We perform calculations on neutral C_7H_8 and $C_{11}H_{12}$ to check whether the CH_2 moiety cuts the current pathway in potentially neutral homoaromatic hydrocarbons because the existence of neutral homoaromatic molecules has been debated.[6,17-19,26,27] The current densities for C_3H_4 and C_3H_6 are studied because cyclopropane is known to sustain a ring current in magnetic fields, even though all its C—C bonds are saturated.[48-50] The current densities are calculated for C_5H_6 and C_6H_8 because they can formally be considered to be homoantiaromatic. Cyclohexane and cyclohexene represent unstrained nonaromatic hydrocarbon rings.

II. Computational Methods

The molecular structures are optimized at the density functional theory (DFT) level using Becke's three-parameter functional combined with the Lee—Yang—Parr exchange-correlation functional (B3LYP) as implemented in TURBOMOLE.[51-53] Calculations of the vibrational frequencies using the AOFORCE program[54] show that the optimized structures are minima on the potential energy surface. The molecular structures are also optimized at the second-order Møller—Plesset perturbation theory (MP2) level. Nuclear magnetic shieldings and magnetically induced current densities are calculated at the B3LYP and MP2 levels.[55-58] The new Karlsruhe triple-ζ basis sets augmented with one set of polarization functions (def2-TZVP) are used.[59-61] The current densities are obtained from the one-particle density matrix and the magnetically perturbed density matrices using the GIMIC approach.[37] The GIMIC method employs gauge-including atomic orbitals (GIAO)[55,62-64] to remove the gauge-origin dependence, to improve the basis-set convergence of the current density, and to reduce errors due to lack of true gauge invariance.[65] A quantitative measure of the aromaticity of the molecules can be deduced from the calculated current densities. The current-density tensor is independent of
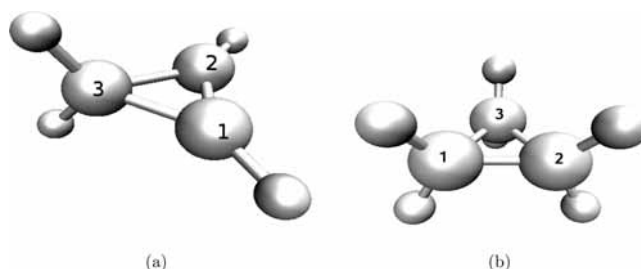

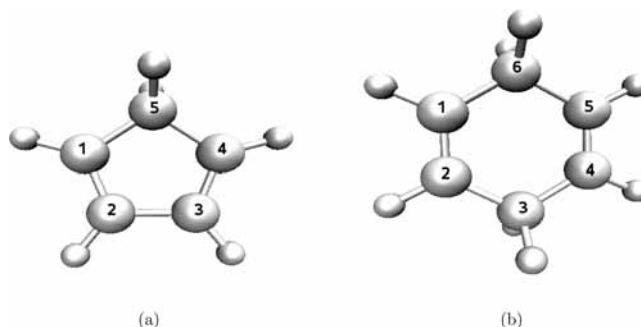**Figure 1.** The optimized molecular structure of (a) C_3H_4 and (b) C_3H_6. The molecular pictures have been made using VMD.[67]

Figure 2. The optimized molecular structure of (a) C_5H_6 and (b) C_6H_8.
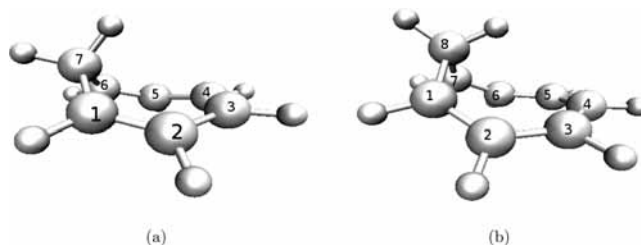

Figure 3. The optimized molecular structure of (a) C_7H_8 and (b) $C_8H_9^+$.

the direction of the magnetic field, whereas the contraction of the tensor with an external magnetic field makes the induced current density direction-dependent. The diatropic and paratropic contributions to the ring-current susceptibilities (ring-current strengths) are obtained by numerical integration of the current density passing through cut planes perpendicular to selected bonds of the molecular rings.[37] The electronic structure calculations are done with TURBOMOLE,[66] whereas the current densities are obtained with GIMIC,[37] which is an independent program that is available on request from the authors.

III. Results

A. Molecular Structures. The optimized molecular structures are depicted in Figures 1, 2, 3, and 4.[67] For all studied molecules except $C_{11}H_{12}$, we obtained only one isomer of relevance for the study. The ruffled and twisted molecular structure of $C_{11}H_{12}$, shown in Figure 4a, is the energetically lowest one. The $C_{11}H_{12}$ isomer in Figure 4b is only 3.5 kJ/mol higher in energy. Calculation of the linking number of the molecular loop[68] yielded a twist value of 1 for the lowest isomer, implying that it has Möbius topology and should with its 10 π electrons be antiaromatic.[69,70] The second $C_{11}H_{12}$ isomer has a twist number of 0.5, and the writhe is 0.5. The bond-length alternation for $C_{11}H_{12}$ is 8−12 pm. The nonvanishing twist numbers of the rings and the strong bond-length alternation indicate that they might lack a continuous electron delocalization path around the ring.
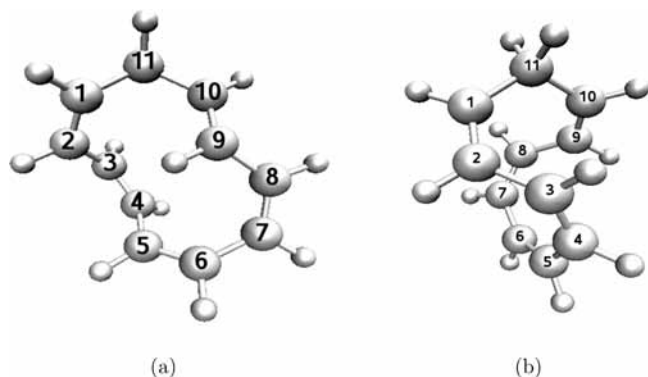
Figure 4. The optimized molecular structure of (a) the lowest $C_{11}H_{12}$ isomer and (b) of the second-lowest $C_{11}H_{12}$ isomer.

TABLE 1: A Comparison of the C−C Distances (in pm) for C_7H_8 Calculated at the B3LYP/def2-TZVP and MP2/ def2-TZVP Levels

method	C_1−C_7	C_1−C_2	C_2−C_3	C_3−C_4	C_1−C_6
B3LYP	150.5	134.5	144.3	135.9	243.7
MP2	149.5	135.7	143.3	137.3	236.7

Homotropylium consists of a rather planar tropylium ($C_7H_7^+$) ring with almost equal carbon−carbon distances and an out-of-plane CH_2 moiety fused to one of the C−C bonds. The C_1−C_7 distance is 214 pm, indicating an attractive interaction between the carbon atoms. The small bond-length alternation for $C_8H_9^+$ suggests that it sustains a stronger ring current than the neutral homoaromatic molecules studied.

Cycloheptatriene has a structure similar to $C_8H_9^+$ and might be an example of a neutral homoaromatic molecule. Calculations of the molecular structure of C_7H_8 show that the C_1−$C_{n−1}$ distance is significantly longer than for $C_8H_9^+$ which might affect its aromaticity because the ring current is expected to cross that gap instead of taking a detour via the CH_2 moiety. To check whether van der Waals interactions shorten the C_1−C_6 distance, we optimized the structure at the MP2 level because dispersion interactions are not well-described at the DFT level with today's functionals. A comparison of the C−C distances of C_7H_8 calculated at the B3LYP and MP2 values is given in Table 1. The table shows that the two computational levels yield almost identical structures having a maximum deviation of about 1−2 pm for the C−C bond lengths. The C−C bonds of the almost planar part of the ring have a bond-length alternation of 10 pm, whereas the C−C bond connecting the CH_2 moiety is a typical single bond of 150 pm. The bond-length alternation is smaller at the MP2 level. The C_1−C_6 distance calculated at the MP2 level is 7 pm shorter than the distance of 244 pm obtained in the B3LYP calculation. The small difference of 7 pm is not expected to have any significant effect on the aromaticity. The C_1−C_6 distance at the B3LYP level is somewhat shorter than the bond distance previously obtained at the DFT level using the generalized gradient approximation.[22] The C_1−C_n distances for the two $C_{11}H_{12}$ isomers are 253 and 255 pm, indicating an even weaker C_1−$C_{n−1}$ interaction. The Cartesian coordinates are given as Supporting Information.

IV. Ring Currents

A. C_6H_6. The computational methods are first applied on benzene, which is here used as the reference aromatic hydrocarbon. The modulus of the current density passing the integration plane at the center of a C−C bond of benzene perpendicularly to the ring is shown in Figure 5a. In the Figure,
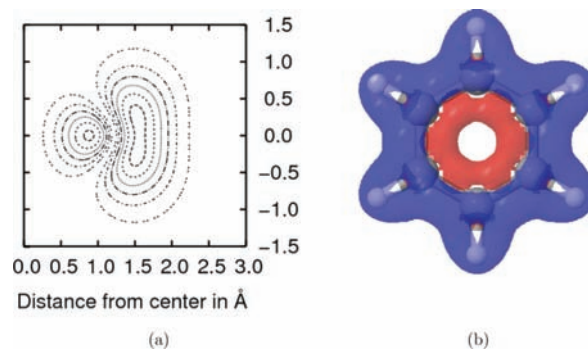

Figure 5. (a) The contour plot (in Å, 1 Å is 100 pm) shows the cross section of the modulus of the ring current of benzene. The benzene ring lies in the *yz* plane. The ring center is at the origin. The C−C bond is perpendicular to the *xy* plane with the center of the bond at $[x, y] = [122, 0.0]$ pm. The smaller cross section area inside the ring corresponds to the paratropic component of the ring current. The larger cross section area mainly outside the benzene ring shows the diatropic contribution to the ring current giving rise to its aromaticity. (b) In the blue region, the current is diatropic and in the red area, it is paratropic. Part b is plotted with Jmol.[71]
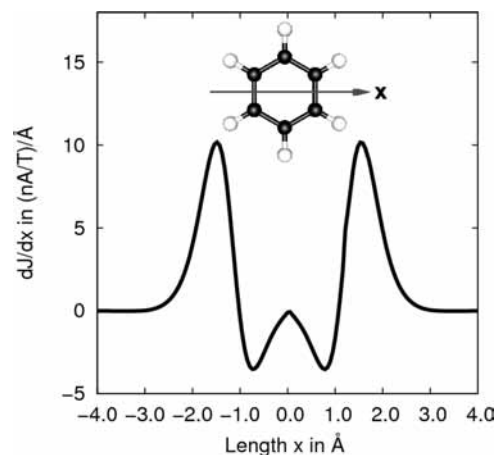

Figure 6. The ring current profile along the arrow passing through a bond of the benzene molecule. The origin is at the center of the ring. The center of the C−C bond is passed at $x = 122$ pm. Paratropic currents are assumed to be negative.

the ring center is at the origin, and the C−C bond is pointing out from the plane of the picture at $[x, y] = [122, 0.0]$ pm. The *y* coordinate denotes the distance from the molecular plane, and *x* is the distance from the ring center. The direction of the external magnetic field is perpendicular to the ring. The contour and modulus plots in Figure 5a and b[71] as well as the ring-current profile in Figure 6 show that a diatropic ring current flows around the molecule on the outside. Inside the benzene ring, the current is paratropic. Qualitatively similar results were obtained in previous studies of the current density for benzene.[37,72,73] Here, we find that the largest current density appears in the molecular plane and not in the π electron density above and below the ring, as generally claimed, whereas Steiner and Fowler[73] estimated that about 80% of the current is transported by the π orbitals. Kutzelnigg et al. noted that addition of the current contributions from the σ and π orbitals destroys the picture of the circular π system.[72] The present current calculations challenge the widespread notion that the ring current is transported by the π electrons on both sides of the ring.[24,74−76] Numerical integration of the current strength passing the C−C bond yields a net current strength of 11.8 nA T^{-1} consisting of a diatropic current of 16.7 nA T^{-1} and a paratropic contribution of −4.9 nA T^{-1}. The net ring-current strength can be used to

Current Densities in Hydrocarbons

J. Phys. Chem. A, Vol. 113, No. 30, 2009 **8671**

TABLE 2: The Diatropic and Paratropic Contributions to the Net Ring Current (in nA T^{-1}) of the Investigated Molecules Calculated at the B3LYP/def2-TZVP Level

molecule	diamagnetic	paramagnetic	total
C_3H_4	11.2	−4.5	6.7
C_3H_6	11.4	−1.4	10.0
C_4H_4	3.5	−23.4	−19.9
C_5H6	11.0	−5.6	5.4
C_6H6	16.7	−4.9	11.8
C_6H_8	9.8	−10.3	−0.5
C_6H_{10}	10.1	−9.6	0.5
C_6H_{12}	7.6	−7.4	0.2
C_7H_8	13.1	−7.0	6.1
$C_8H_9{}^+$	18.1	−5.2	12.9
$C_{11}H_{12}{}^a$	10.2	−8.0	2.2
$C_{11}H_{12}{}^b$	11.4	−7.0	4.4

^{a} The lowest isomer. ^{b} The second-lowest isomer.

Figure 8. (a) The contour plot (in Å) shows the cross section of the modulus of the ring current of C_3H_6. The ring lies in the yz plane. The ring center is at the origin. The C−C bond is perpendicular to the xy plane with the center of the bond at $[x, y]=[44, 0.0]$ pm. The smaller cross section area inside the ring corresponds to the paratropic component of the ring current. The larger cross section area outside the ring shows the diatropic contribution to the ring current. (b) In the blue region, the current is diatropic, and in the red area, it is paratropic. Part b is plotted with Jmol.[71]
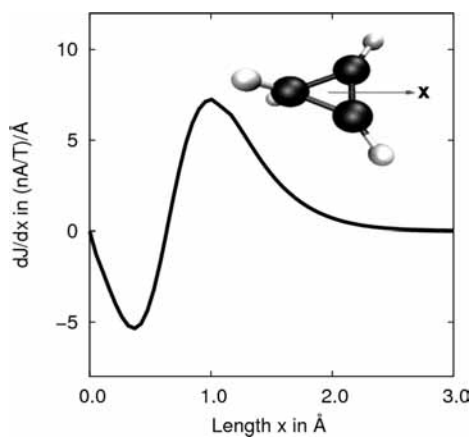

Figure 7. The ring current profile of C_3H_4 along the arrow and passing through the double bond opposite the CH$_2$ group. The origin is at the center of the molecular ring. The C_1-C_2 bond is passed at 68 pm. Paratropic currents are assumed to be negative.

Figure 9. The ring current profile of C_3H_6 along the arrow passing through the single bond opposite the CH$_2$ group. The origin is at the center of the molecular ring. The C_1-C_2 bond is passed at 65 pm. Paratropic currents are assumed to be negative.

define an aromaticity index. A linear aromaticity scale can be constructed with 11.8 nA/T for benzene as the reference point for an aromatic molecule and the zero net ring current as the reference value for nonaromatic molecules. The calculated ring-current strengths are summarized in Table 2.

B. C_3H_4. The net ring current passing the C−C bonds of cyclopropene is 6.7 nA T^{-1}, which is roughly half the benzene value. The diatropic ring current flows on the outside of the molecule, and it is strongest in the molecular plane. A weaker paratropic current circles inside the three-membered ring. The ring current profile starting at the center of the molecular ring and passing the double bond is displayed in Figure 7. It verifies that the diatropic contribution to the ring current dominates outside the ring, whereas the current is paratropic inside the ring, as for benzene.

The paratropic contribution to the ring current of −1.8 nA T^{-1} passing the single bonds is less than half the strength of the paratropic current of −4.5 nA T^{-1} at the double bond. The *bond current* of the double bond is stronger than for the single bond because of a more extensive electron delocalization. The ring current of C_3H_4 can be considered to consist of diatropic and paratropic ring currents circling around the whole ring and of three diatropic bond currents. Thus, the paratropic ring current can to some extent be considered as a consequence of the diatropic currents circling locally around the bonds. For molecules with little bond alternation and largely equal bond-current strengths, the bond current contributions to the diatropic and paratropic currents can be considered to vanish because all
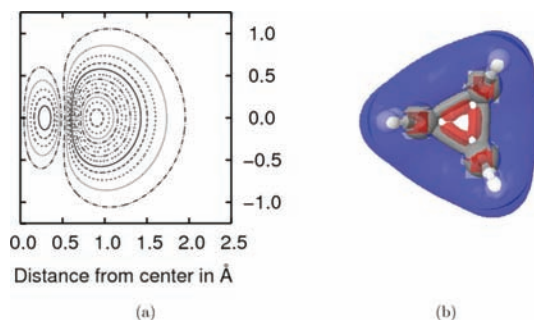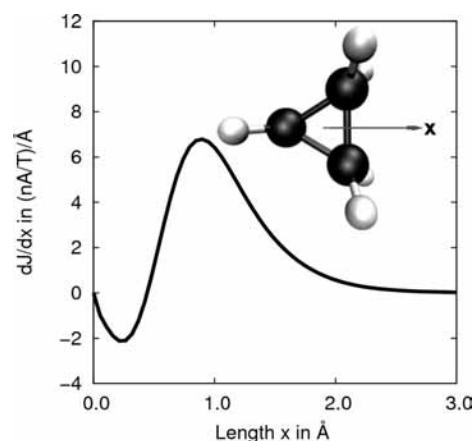
bonds have the same current strength. The bond currents are local and do not affect the net ring-current strength. The current density circling around ethen and ethyn has recently been studied by Pelloni and Lazzeretti.[77]

C. C_3H_6. Cyclopropane does not fulfill any structural criteria for aromatic molecules. It is included in this study because it has been shown to sustain ring currents when exposed to external magnetic fields.[48−50] Its ring current is not negligible because the total current strength is 10.0 nA T^{-1}, which is only 1.8 nA T^{-1} smaller than for benzene. The contour and modulus plots in Figure 8 as well as the current profile in Figure 9 show that the diatropic current flows on the outside of the ring and small paratropic current circles inside it. The strongest current density appears in the molecular plane. The cross section area of the current density passing the integration plane at the center of the C−C bond resembles that of benzene, and the current strength in the molecular plane of benzene and cyclopropane are of about the same size. On the basis of their current calculations, Pelloni, Lazzeretti, and Zanasi concluded that cyclopropane does not sustain any exceptionally strong σ current.[48] They found that the strength of the σ current is of the same size as the current flow in the molecular plane of benzene. However, they did not report any current strengths.[48] Our calculations of the current strengths show that the strongest diatropic current flow appears in the molecular plane for both
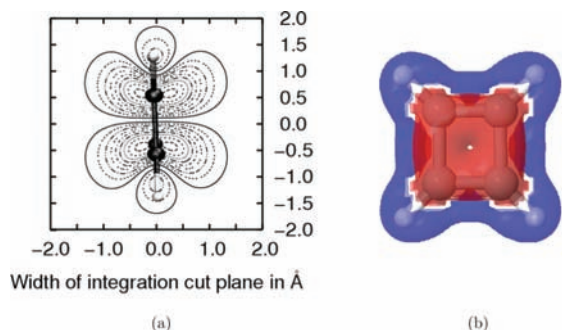
Figure 10. (a) The contour plot (in Å) shows the cross section of the modulus of the ring current of C_4H_4. The ring lies in the yz plane. The smaller cross section area outside the ring corresponds to the diatropic component of the ring current. The larger cross section area inside the ring shows the paratropic contribution to the ring current. The $C-C$ single bonds are perpendicular to the xy plane at $[x, y] = [0.0, 67]$ pm. (b) In the blue region, the current is diatropic, and in the red area, it is paratropic. Part b is plotted with Jmol.[71]

Figure 11. The contour plot (in Å) shows the cross section of the modulus of the ring current of C_5H_6. The molecule lies in the yz plane. The cross section plane cutting the whole molecule is perpendicular to the C_1-C_4 axis and passes 26 pm from the carbon of the CH_2 group.

molecules, and the numerical integration of the net current strength yields almost the same current strength for cyclopropane as obtained for benzene. Thus, according to the ring-current criterion, C_3H_6 is almost as aromatic as benzene, even though it is fully saturated. Cremer et al. found that the σ delocalization compensates the ring strain and stabilizes the molecule.[78,79] Dewar and Cremer found in thier studies that the σ conjugation and σ delocalization in C_3H_6 corresponds to the π conjugation and π delocalization in benzene and concluded that cyclopropene is σ-aromatic.[80,81]

The ring strain seems to make the electrons mobile, resulting in a strong magnetic ring current, which could be called *ring-strain current*, affecting magnetic shieldings in the same way as ring currents do. The cross section area for the diatropic current at the center of the $C-C$ bond is somewhat less outstretched for C_3H_6 than for benzene due to the absence of occupied π orbitals at the single bond. However, a well-defined distinction between σ and π aromaticity cannot be seen by comparing the contour plots for benzene and cyclopropane in Figures 5 and 8.

C. C_4H_4. The current calculations on the antiaromatic cyclobutadiene molecule yield a strong net paratropic ring current of -19.9 nA T^{-1} at the double bond. The contour and modulus plots in Figure 10 show that the dominating paratropic ring current flows inside the ring with the largest current density in the ring plane, whereas the much weaker diatropic ring current of 3.5 nA T^{-1} circles on the outside of the molecule, also mainly in the ring plane. For the single bond, the strengths of the paratropic and diatropic currents are -22.7 and 2.7 nA T^{-1}, respectively, yielding a strong net paratropic ring current of -20.0 nA T^{-1}, as expected for an antiaromatic molecule.

E. C_5H_6. The 1,3-cyclopentadiene molecule could formally be considered homoantiaromatic with a CH_2 moiety fused into the antiaromatic cyclobutadiene molecule, cutting the conjugation pathway similarly to CH_2 in $C_8H_9^+$. The formal homoantiaromatic C_5H_6 molecule sustains diatropic and paratropic currents of 11.0 and -5.6 nA T^{-1}, yielding a total diatropic current of 5.4 nA T^{-1}. Thus, according to the ring current criterion, C_5H_6 would be weakly aromatic. Apparently, the ring strain increases the electron mobility in the unconjugated C_5H_6 ring, giving rise to a net diatropic ring current. The dominating diatropic current flows outside the molecular ring, and a smaller paratropic one circles inside it. Figure 11 shows a contour profile of the modulus of the ring current passing through the whole C_5H_6 molecule. The molecule lies in the xz plane with the cross
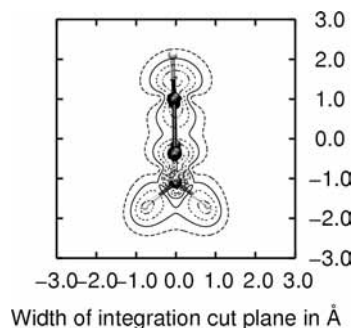
section surface perpendicularly to the C_1-C_4 axis. The cross section plane cuts the C_1-C_5 single bond 26 pm from the carbon atom. The calculations show that the diatropic current passes the CH_2 moiety in the vicinity of the hydrogens, and the paratropic current takes the inner route. The CH_2 group does not interrupt the current flow. Neither does the diatropic current make a short cut from C_1 to C_4, as suggested for homoaromatic molecules.

F. C_6H_8, C_6H_{10}, and C_6H_{12}. The 1,4-cyclohexadiene molecule could formally be considered as a doubly homoantiaromatic hydrocarbon with two CH_2 moieties fused into the antiaromatic cyclobutadiene molecule. The current density calculations on C_6H_8 shows that it sustains diatropic and paratropic ring currents of 9.8 and -10.3 nA T^{-1}, respectively. The current contributions cancel, yielding a very weak paratropic ring current of -0.5 nA T^{-1}, as prevously reported.[45] Cyclohexene and cyclohexane also sustain ring currents. Their diatropic and paratropic currents are of the same size and cancel. For C_6H_{12}, the net current is 0.2 nA T^{-1} consisting of diatropic and paratropic contributions of 7.6 and -7.4 nA T^{-1}, respectively. For C_6H_{10}, the corresponding values are 10.1, -9.6, and 0.5 nA T^{-1}. The ring current is much smaller for the unconjugated six-membered rings than for the smaller rings because the ring strain decreases with increasing ring size. For C_6H_{10} and C_6H_{12}, the net current is weakly diatropic, whereas for C_6H_8, the net ring current is slightly paratropic, which might or might not be a consequence of its formally double homoantiaromaticty character. Because these molecules sustain diatropic and paratropic currents of equal strength leading to a vanishing net ring current strength, they can be considered nonaromatic.

G. C_7H_8. The 1,3,5-cycloheptatriene molecule is nonplanar with the exo hydrogen of the CH_2 moiety outside the molecular ring and the endo hydrogen inside it. The measured ^{1}H NMR chemical-shift difference between the endo and exo hydrogens is 1.38 ppm,[75] which is in perfect agreement with the calculated value of 1.36 ppm at the B3LYP level. The magnetic shielding is smaller for H(exo) than for H(endo), suggesting that a diatropic ring current is sustained by the molecule. The ^{1}H NMR shieldings calculated at different levels are compared to experimental values in Table 3. The difference in the shieldings of H(exo) and H(endo) is slightly underestimated at the Hartree–Fock self-consistent field (HF SCF) level, whereas the MP2 calculations yield somewhat too large values as compared to experiment. The ^{1}H NMR chemical shifts of H(exo) and H(endo) calculated at the HF SCF, MP2 and B3LYP levels agree within 0.36 ppm with the experimental values. The tiny difference is mainly due to vibrational, temperature, and solvent effects, which were not considered in the calculations. Basis-

Current Densities in Hydrocarbons

J. Phys. Chem. A, Vol. 113, No. 30, 2009 **8673**

TABLE 3: Comparison of Experimental and Calculated Chemical Shifts of H(endo) and H(exo) As Well As the Corresponding Chemical Shift Differences ($\Delta\delta_{endo-exo}$) for C_7H_8 and $C_8H_9^{+a}$

level	C_7H_8			$C_8H_9^+$		
chemical shift	$\Delta\delta_{endo-exo}$	δ_{endo}	δ_{exo}	$\Delta\delta_{endo-exo}$	δ_{endo}	δ_{exo}
HF SCF/def2-TZVP	1.09	1.58	2.67	5.71	−0.83	4.88
MP2/def2-TZVP	1.55	1.50	3.05	6.53	−1.22	5.31
B3LYP/def2-TZVP	1.36	1.67	3.03	5.86	−0.69	5.20
experiment[b]	1.38	1.31	2.69	5.89	−0.73	5.13

[a] The ^1H NMR chemical shifts are calculated at different levels using the B3LYP/def2-TZVP molecular structure. TMS is used as reference compound. All values in parts per million. [b] Refs 75 (C_7H_8) and 47 ($C_8H_9^+$).

set, electron-correlation, and geometric effects are also possible sources for the small difference between experimental and computed shifts.

The C−C bond lengths of the formal single and double bonds in C_7H_8 slightly alternate. As a result, calculations also show stronger para- and diatropic contributions to the current at the center of the formal double bonds than for the single bonds. This implies that the external magnetic field induces stronger local currents around the formal double C−C bonds than for the single bonds. The bond currents are stronger for the double bonds with delocalized π electrons. The sum of the diatropic and paratropic contributions is independent of the position of the integration plane. Small variations in the current strength depending the position of the plane can appear in the calculations due to numerical inaccuracies and the use of finite basis sets.[37] The strength of the diatropic and paratropic ring currents at the B3LYP level are 13.1 and −7.0 nA T^{-1}, respectively. The strength of the net ring current for C_7H_8 is 6.1 nA T^{-1}, which is about half the benzene value suggesting that it, despite the bridging CH_2 moiety being half as aromatic as benzene.

Calculations of the current density at the MP2 level were performed to check whether dispersion interactions play a role. The diatropic and paratropic currents are 15.0 and −6.8 nA T^{-1}, respectively. At the MP2 level, the net ring-current strength is 8.2 or 2.1 nA T^{-1} larger than the DFT value. The van der Waals interaction shortens the C_1−C_6 distance by 7 pm, and the MP2 structure has a smaller bond-length alternation, leading to a somewhat larger ring current. Herges and Geuenich[23] calculated the ring current for C_7H_8 and visualized the current by using their anisotropy of the current-induced density (ACID) approach.[23,24] The current plot confirmed a through-space interaction between C_1 and C_6, forming a homoaromatic molecule. The present current calculations show that the current taking the shortest short-cut route is paratropic. The diatropic current follows mainly the C−C bond toward the CH_2 moiety.

Figure 12 shows a contour plot of the modulus of the ring current passing the whole molecule. The cross section plane lies in the xy plane perpendicularly to the C_1−C_6 axis and passes 0.26 pm from the carbon of the CH_2 unit. It shows that the ring current passes at the hydrogens of the CH_2 moiety and on the inside of the carbon. The current cross section at the C_3−C_4 bond has a diatropic part outside the ring and a smaller paratropic area inside it, as for benzene. The current cross section is distorted by the CH_2 group which is breaking the planar symmetry of the molecule. The ring current profile through the whole molecule is shown in Figure 13. The negative peaks have their minima less than 100 pm from the ring center, indicating that the paratropic ring current circles inside the ring and passes through the space from C_1 to C_6. The diatropic and paratropic
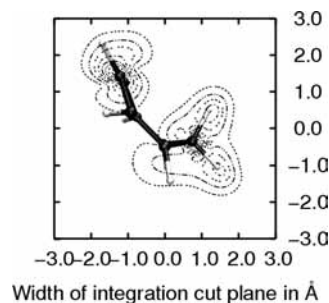

Figure 12. The contour plot (in Å) shows the cross section of the modulus of the ring current of C_7H_8. The cross section plane cutting the whole molecule is perpendicular to the C_1−C_6 axis and passes 26 pm from the carbon of the CH_2 group.
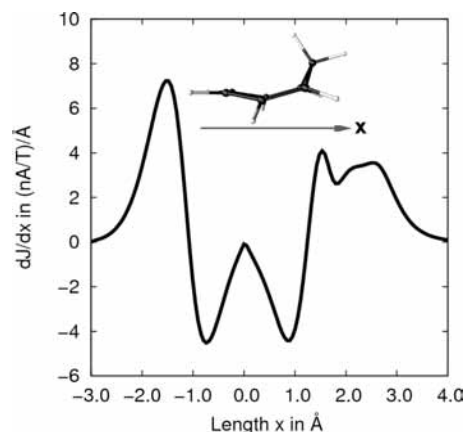

Figure 13. The ring current profile of C_7H_8 along the arrow and passing at $x = -124$ pm through the C_3−C_4 bond opposite to the CH_2 group. The origin is at the center of the molecular ring. Paratropic currents are assumed to be negative.

ring currents are spatially separated. The diatropic currents circle mainly on the outside of the molecular ring. The double peak structure in Figure 13 shows that the diatropic current branches out into an outer route, passing the hydrogens of the CH_2 moiety and to a weaker current inside it. The CH_2 group does not interrupt the current flow around the ring. Thus, the current calculations challenge the accepted notion that the diatropic ring current makes a short cut from C_1 to C_{n-1} in homoaromatic molecules.

H. $C_8H_9^+$. The archetypal homoaromatic molecule is homotropylium. It has a nearly planar structure for the tropylium part with the CH_2 moiety out of the plane. The endo hydrogen lies inside the ring and H(exo) outside it, as for C_7H_8. The ring current increases the ^1H NMR shielding of H(endo), and the H(exo) shielding becomes smaller. The measured ^1H NMR chemical-shift difference between the endo and exo hydrogens is 5.86 ppm,[5,6,47] which is in excellent agreement with the present B3LYP value of 5.89 ppm. In Table 3, the measured H(endo) and H(exo) chemical shifts and the chemical-shift differences are compared with values obtained at different computational levels. The chemical shifts calculated at the B3LYP level agree slightly better with measured values than the MP2 ones.

The ^1H NMR resonances for H(endo) and H(exo) measured for a homotropylium salt appear at $\delta_{endo} = -0.73$ ppm and $\delta_{exo} = 5.13$ ppm relative to tetramethylsilane (TMS).[46] These values can be compared to the corresponding chemical shifts of −0.69 and 5.20 ppm calculated at the B3LYP level for an isolated $C_8H_9^+$ molecule. The large shielding difference between H(endo) and H(exo) indicates that $C_8H_9^+$ sustains a strong net diatropic ring current. The small bond-length alternation and the planarity

8674 *J. Phys. Chem. A, Vol. 113, No. 30, 2009*
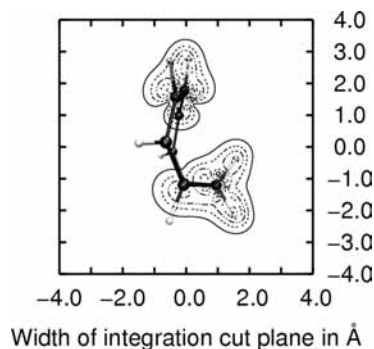
Fliegl et al.

Figure 14. The contour plot (in Å) shows the cross section of the modulus of the ring current of $C_8H_9^+$. The cross section plane cutting the whole molecule is perpendicular to the C_1-C_7 axis and passes 26 pm from the carbon of the CH_2 group.
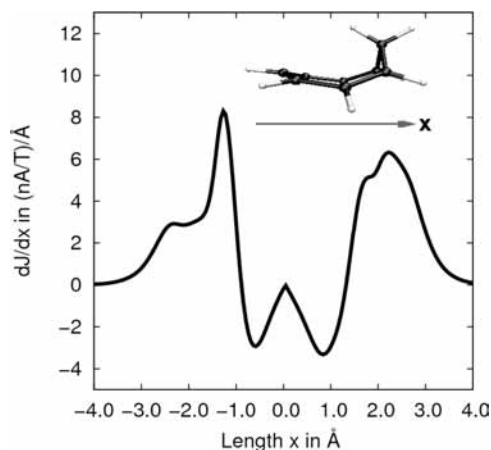

Figure 15. The ring current profile of $C_8H_9^+$ along the arrow and passing at $x = -161$ pm through C_3-C_4 bond opposite the CH_2 group. The origin is at the center of the molecular ring. Paratropic currents are assumed to be negative.

of the $C_7H_7^+$ part of the ring indicates that it sustains a magnetically induced ring current, as also found in the study by Cremer et al.[12] Because the distance of 149 pm between the $C_7H_7^+$ part and the CH_2 moiety is typical for a single C—C bond, one has assumed that the current path does not involve the CH_2 moiety. The current has been expected to pass from C_1 to C_7 without taking a detour via the CH_2 group.[82]

Figure 14 shows the contour of the current passing a cross section through the whole molecule and passes 26 pm from the carbon of the CH_2 group. The cross section in the xy plane is perpendicular to the C_1-C_7 axis. The current cross section area at the C_3-C_4 bond opposite to the CH_2 group looks like the one obtained for benzene: a large diatropic contribution outside the molecular ring and a small paratropic one inside it with the strongest current density in the ring plane. The shape of the cross section is slightly distorted due to the presence of the CH_2 moiety. The shape of the ring current flowing around molecule and passing a plane perpendicularly to the C_1-C_7 axis is shown in Figure 15. The negative peaks corresponding to the paramagnetic ring current have minima about ±100 pm from the ring center. The paratropic current flows inside the ring and passes through the space from C_1 to C_7 without taking the detour via the CH_2 moiety. The diatropic current flows on the outside of the molecular ring. The diatropic current follows the C_1-C_8 single bond and passes on both sides of the CH_2 group. The diatropic current is stronger on the outside of the CH_2 moiety than inside it.

Integration of the current density passing half the molecule through the plane yields a strong diatropic ring current of 18.1 nA T^{-1} and a paratropic contribution of -5.2 nA T^{-1}. The net ring current strength of 12.9 nA T^{-1} is of the same size as that obtained for benzene. The current calculations confirm that $C_8H_9^+$ is a homoaromatic molecule.

I. $C_{11}H_{12}$. For 1,3,5,7,9-*cyclo*-undecapentaene, we obtain two low-lying isomers separated by only 3.5 kJ/mol. Calculations of the topology of the isomers yielded linking numbers of 1 for both. The energetically lower isomer is a Möbius molecule having a twist number of nearly 1 and an almost vanishing writhe. The sum of the twist and writhe numbers is equal to the linking number.[68] The second isomer of C_2 symmetry has twist and writhe numbers of about 0.5. For nonplanar molecules, such as $C_{11}H_{12}$, it is sometimes a challenge to choose the position and size of the cut plane such that the integration procedure captures the whole current that passes the studied bond without considering current contributions from other parts of the molecule. The choice of the direction of the magnetic field is not obvious, either. We have chosen a magnetic field direction that yields largely the maximum projection area of the molecular ring perpendicular to the field. Integration of the current passing a plane cutting the C_1-C_{11} bond yielded a ring-current strength of 2.2 nA T^{-1}. For the energetically higher-lying isomer, the net ring current is 4.4 nA T^{-1}. The net ring currents consist of a strong diatropic current on the outside, which is partially canceled by the paratropic flow inside the ring. The diatropic contributions are 10.2 and 11.4 nA T^{-1}, whereas the strengths of the paratropic currents are -8.0 and -7.0 nA T^{-1} for the lowest and second-lowest isomers, respectively. The Möbius twist of the lowest isomer does not prevent or reverse the current flow; it reduces the current strength to half the value of the less twisted isomer.

V. Summary and Discussion

The magnetically induced current densities of hydrocarbon rings have been investigated at the B3LYP DFT level using gauge-including atomic orbitals. The current densities were obtained using the gauge-including magnetically induced current (GIMIC) method. The ring-current (current susceptibility) strengths were obtained by numerical integration of the current density passing cross section planes through C—C bonds. The calculated ring-current strengths are summarized in Table 2.

The current density calculations show that strong paratropic and diatropic currents are sustained in the studied molecules. For benzene, the diatropic contribution to the ring current flows on the outside of the molecule, mainly in the molecular plane and not in the π cloud, as previously believed. The ring current has a weaker paratropic component on the inside of the benzene ring, resulting in the net diatropic ring current that is typical for aromatic molecules. For cyclobutadiene, which is an antiaromatic molecule, the paratropic current inside the ring dominates. For the nonaromatic six-membered rings with unconjugated and saturated C—C bonds, the diatropic current outside the ring and the paratropic one inside it have the same strength with opposite sign and cancel. For small unconjugated and saturated hydrocarbon rings, strong net ring currents are induced by external magnetic fields. The total ring current of cyclopropene, cyclopropane, and 1,3-cyclopentadiene are 6.7, 10.0, and 5.4 nA T^{-1}, respectively. These values can be compared to the current strength of 11.8 nA T^{-1} for benzene. The ring strain of the three-membered ring increases the electron mobility, giving rise to a ring-strain current. The ring-strain current affects the magnetic shieldings in the same way as the

Current Densities in Hydrocarbons

J. Phys. Chem. A, Vol. 113, No. 30, 2009 **8675**

aromatic ring current does. Magnetic shielding calculations cannot distinguish between aromatic and strain currents, which might be a reason why different aromaticity criteria sometimes yield different degrees of aromaticity.[28−33]

The net ring current of cycloheptatriene is 6.1 nA T^{-1}, which is roughly half the benzene value. The molecule can be considered slightly aromatic according to the ring current criterion. The homotropylium cation, which is known to be homoaromatic, has a ring current of 12.9 nA T^{-1}. The contour plots and the current profile obtained with the integration plane in the vicinity of the CH$_2$ group show that the diatropic current takes a detour via the CH$_2$ moiety, whereas the paratropic one takes a shorter route from C$_1$ to C$_{n-1}$. The current calculations on the homoaromatic molecules show that the CH$_2$ group does not interrupt the current flows around the ring. The diatropic current flow along the single bond to the CH$_2$ group, where it splits into an outer route passing the hydrogens of the CH$_2$ moiety and a weaker current, flows inside the carbon atom. For homoaromatic molecules, the diatropic ring current does not take the short-cut route C$_1$ to C$_{n-1}$, as one previously believed.

The ring current strength of the Möbius twisted isomer of *cyclo*-undecapentaene is 2.2 nA T^{-1}. Ring-current calculations show that the energetically lowest isomer is very weakly aromatic, sustaining a ring current that is about 20% of the benzene value. The aromaticity rule for Möbius molecules implies that it should, in fact, be homoantiaromatic because it is Möbius-twisted with a twist number of 1 and possesses 10 π electrons. The second-lowest isomer of *cyclo*-undeca-pentaene has a ring current strength of 4.4 nA T^{-1}. It is less twisted, with a twist number of 0.5. The linking number of both isomers is 1.

Supporting Information Available: The Cartesian coordinates of the molecular structures. This material is available free of charge via the Internet at http://pubs.acs.org.

References and Notes

(1) Shelby, R. A.; Smith, D. R.; Schultz, S. *Science* **2001**, *292*, 77–79.
(2) Linden, S.; Enkrich, C.; Wegener, M.; Zhou, J.; Koschny, T.; Soukoulis, C. M. *Science* **2004**, *306*, 1351–1353.
(3) Busch, K.; von Freymann, S. L. G.; Mingaleev, S. F.; Tkeshelash-vili, L.; Wegener, M. *Phys. Rep.* **2007**, *444*, 101–202.
(4) Winstein, S. *J. Am. Chem. Soc.* **1959**, *81*, 6524–6525.
(5) Childs, R. F. *Acc. Chem. Res.* **1984**, *17*, 347–352.
(6) Williams, R. V. *Chem. Rev.* **2001**, *101*, 1185–1204.
(7) Jorgensen, W. L. *J. Am. Chem. Soc.* **1976**, *98*, 6784–6789.
(8) Kaufmann, E.; Mayr, H.; Chandrasekhar, J.; von Ragué Schleyer, P. *J. Am. Chem. Soc.* **1981**, *103*, 1375–1380.
(9) Grutzner, J. B.; Jorgensen, W. L. *J. Am. Chem. Soc.* **1981**, *103*, 1372–1375.
(10) Haddon, R. C. *J. Am. Chem. Soc.* **1988**, *110*, 1108–1112.
(11) Svensson, P.; Reichel, F.; Ahlberg, P.; Cremer, D. *J. Chem. Soc. Perkin Trans. 2* **1991**, 1463–1469.
(12) Cremer, D.; Reichel, F.; Kraka, E. *J. Am. Chem. Soc.* **1991**, *113*, 9459–9466.
(13) Willershausen, R. P.; Kybart, C.; Stamatis, N.; Massa, W.; Bühl, M.; von Ragué Schleyer, P.; Berndt, A. *Angew. Chem., Int. Ed.* **1992**, *31*, 1238–1240.
(14) Cremer, D.; Svensson, P.; Kraka, E.; Konkoli, Z.; Ahlberg, P. *J. Am. Chem. Soc.* **1993**, *115*, 7457–7464.
(15) Jiao, H.; van Eikema Hommes, N. J. R.; von Ragué Schleyer, P.; de Meijere, A. *J. Org. Chem.* **1996**, *61*, 2826–2828.
(16) Nishinaga, R. T.; Izukawa, Y.; Komatsu, K. *J. Phys. Org. Chem.* **1998**, *11*, 475–477.
(17) Houk, K. N.; Wells Gandour, R.; Strozier, R. W.; Rondan, N. G.; Paquette, L. A. *J. Am. Chem. Soc.* **1979**, *101*, 6797–6802.
(18) Williams, R. V.; Kurtz, H. A. *J. Org. Chem.* **1988**, *53*, 3626–3628.
(19) Donovan, W. H.; White, W. E. *J. Org. Chem.* **1996**, *61*, 969–977.
(20) Lepetit, C.; Godard, C.; Chauvin, R. *New J. Chem.* **2001**, *25*, 572–580.
(21) Scheschkewitz, D.; Hofmann, M.; Ghaffari, A.; Amseis, P.; Präsang, C.; Mesbah, W.; Geiseler, G.; Massa, W.; Berndt, A. *J. Organomet. Chem.* **2002**, *646*, 262–270.
(22) Jusélius, J.; Patzschke, M.; Sundholm, D. *J. Mol. Struct. (Theochem)* **2003**, *633*, 123–136.
(23) Herges, R.; Geuenich, D. *J. Phys. Chem. A* **2001**, *105*, 3214–3220.
(24) Geuenich, D.; Hess, K.; Kohler, F.; Herges, R. *Chem. Rev.* **2005**, *105*, 3758–3772.
(25) Chen, Z.; Jiao, H.; Wu, J. I.; Herges, R.; Zhang, S. B.; von Ragué Schleyer, P. *J. Phys. Chem. A* **2008**, *112*, 10586–10594.
(26) Stahl, F.; von Rague Schelyer, P.; Jiao, H.; Schaefer, H. F.; Chen, K. H.; Allinger, N. L. *J. Org. Chem.* **2002**, *67*, 6599–6611.
(27) Fowler, P. W.; Lillington, M.; Olson, L. P. *Pure Appl. Chem.* **2007**, *79*, 969–979.
(28) Katritzky, A. R.; Barczyński, P.; Musumarra, G.; Pisano, D.; Szafran, M. *J. Am. Chem. Soc.* **1989**, *111*, 7–15.
(29) Neus, J. *Aromatizität: Geschichte und mathematische Analyse eines fundamentalen chemischen Begriffs*; HYLE Publications: Karlsruhe, 2002.
(30) Jug, K.; Köster, A. *J. Phys. Org. Chem.* **1991**, *4*, 163–169.
(31) Krygowski, T. M.; Ciesielski, R.; Bird, C. W.; Kotschy, A. *J. Chem. Inf. Comput. Sci.* **1995**, *35*, 203–210.
(32) von Ragué Schleyer, P.; Freeman, P. K.; Jiao, H.; Goldfuss, B. *Angew. Chem., Int. Ed.* **1995**, *34*, 337–340.
(33) Bird, C. W. *Tetrahedron* **1996**, *52*, 9945–9952.
(34) Fias, S.; Fowler, P. W.; Delgado, J. L.; Hahn, U.; Bultinck, P. *Chem.−Eur. J.* **2008**, *14*, 3093–3099.
(35) Taubert, S.; Jusélius, J.; Sundholm, D.; Klopper, W.; Fliegl, H. *J. Phys. Chem. A* **2008**, *112*, 13584–13592.
(36) Jusélius, J.; Sundholm, D. *Phys. Chem. Chem. Phys.* **2008**, *10*, 6630–6634.
(37) Jusélius, J.; Sundholm, D.; Gauss, J. *J. Chem. Phys.* **2004**, *121*, 3952–3963.
(38) Zanasi, R.; Lazzeretti, P.; Malagoli, M.; Piccinini, F. *J. Chem. Phys.* **1995**, *102*, 7150–7157.
(39) Lazzeretti, P. *Prog. Nucl. Magn. Reson. Spectrosc.* **2000**, *36*, 1–88.
(40) Gomes, J. A. N. F.; Mallion, R. B. *Chem. Rev.* **2001**, *101*, 1349–1384.
(41) Lin, Y. C.; Jusélius, J.; Sundholm, D.; Gauss, J. *J. Chem. Phys.* **2005**, *122*, 214308.
(42) Lin, Y. C.; Sundholm, D.; Jusélius, J.; Cui, L. F.; Li, X.; Zhai, H. J.; Wang, L. S. *J. Phys. Chem. A* **2006**, *110*, 4244–4250.
(43) Johansson, M. P. *J. Phys. Chem. C* **2009**, *113*, 524–530.
(44) Johansson, M. P.; Jusélius, J. *Lett. Org. Chem.* **2005**, *2*, 469–474.
(45) Johansson, M. P.; Jusélius, J.; Sundholm, D. *Angew. Chem., Int. Ed.* **2005**, *44*, 1843–1846.
(46) von Rosenberg, J. L., Jr.; Mahler, J. E.; Petit, R. *J. Am. Chem. Soc.* **1962**, *84*, 2842–2843.
(47) Warner, P.; Harris, D. L.; Bradley, C. H.; Winstein, S. *Tetrahedron Lett.* **1970**, *11*, 4013–4016.
(48) Pelloni, S.; Lazzeretti, P.; Zanasi, R. *J. Phys. Chem. A* **2007**, *111*, 8163–8169.
(49) Göller, A.; Clark, T. *J. Mol. Model.* **2000**, *6*, 133–149.
(50) Fowler, P. W.; Baker, J.; Lillington, M. *Theor. Chem. Acc.* **2007**, *118*, 123–127.
(51) Becke, A. D. *J. Chem. Phys.* **1993**, *98*, 5648–5652.
(52) Lee, C.; Yang, W.; Parr, R. G. *Phys. Rev. B* **1988**, *37*, 785–789.
(53) Ahlrichs, R.; Bär, M.; Häser, M.; Horn, H.; Kölmel, C. *Chem. Phys. Lett.* **1989**, *162*, 165–169; for the current version, see: http://www.turbomole.com.
(54) Deglmann, P.; Furche, F. *Chem. Phys. Lett.* **2002**, *362*, 511–518.
(55) Wolinski, K.; Hinton, J. F.; Pulay, P. *J. Am. Chem. Soc.* **1990**, *112*, 8251–8260.

8676 *J. Phys. Chem. A, Vol. 113, No. 30, 2009*

Fliegl et al.

(56) Häser, M.; Ahlrichs, R.; Baron, H. P.; Weis, P.; Horn, H. *Theor. Chim. Acta* **1992**, *83*, 455–470.

(57) Kollwitz, M.; Häser, M.; Gauss, J. *J. Chem. Phys.* **1998**, *108*, 8295–8301.

(58) Gauss, J. *Chem. Phys. Lett.* **1992**, *191*, 614–620.

(59) Schäfer, A.; Horn, H.; Ahlrichs, R. *J. Chem. Phys.* **1992**, *97*, 2571–2577.

(60) Schäfer, A.; Huber, C.; Ahlrichs, R. *J. Chem. Phys.* **1994**, *100*, 5829–5835.

(61) Weigend, F.; Ahlrichs, R. *Phys. Chem. Chem. Phys.* **2005**, *7*, 3297–3305.

(62) London, F. *J. Phys. Radium* **1937**, *8*, 397–409.

(63) Hameka, H. F. *Mol. Phys.* **1958**, *1*, 203–215.

(64) Ditchfield, R. *Mol. Phys.* **1974**, *27*, 789–807.

(65) Epstein, S. T. *J. Chem. Phys.* **1973**, *58*, 1592–1595.

(66) Ahlrichs, R.; Bär, M.; Häser, M.; Horn, H.; Kölmel, C. *Chem. Phys. Lett.* **1989**, *162*, 165–169.

(67) Humphrey, W.; Dalke, A.; Schulten, K. *J. Mol. Graphics* **1996**, *14*, 33–38.

(68) Rappaport, S. M.; Rzepa, H. S. *J. Am. Chem. Soc.* **2008**, *130*, 7613–7619.

(69) Heilbronner, E. *Tetrahedron Lett.* **1964**, *5*, 1923–1928.

(70) Zimmerman, H. E. *J. Am. Chem. Soc.* **1966**, *88*, 1564–1565.

(71) *JMOL: an open-source Java viewer for chemical structures in 3D*; http://www.jmol.org.

(72) Kutzelnigg, W.; van Wüllen, C.; Fleischer, U.; Franke, R.; van Mourik, T. In *Nuclear Magnetic Shieldings and Molecular Structure*; Tossell, J. A., Ed.; Kluwer Academic Publishers: Dordrecht, The Netherlands, 1993; pp 141−161.

(73) Steiner, E.; Fowler, P. W. *Int. J. Quantum Chem.* **1996**, *60*, 609–616.

(74) Heine, T.; Islas, R.; Merino, G. *J. Comput. Chem.* **2007**, *28*, 302–309.

(75) Günther, H. *NMR Spectroscopy: Basic Principles, Concepts, and Applications in Chemistry*, 2nd ed.; John Wiley & Sons: New York, 1995.

(76) Soncini, A.; Fowler, P. W.; Lazzeretti, P.; Zanasi, R. *Chem. Phys. Lett.* **2005**, *401*, 164–169.

(77) Pelloni, S.; Lazzeretti, P. *Chem. Phys.* **2009**, *356*, 153–163.

(78) Cremer, D.; Gauss, J. *J. Am. Chem. Soc.* **1986**, *108*, 7476–7477.

(79) Cremer, D.; Kraka, E. *J. Am. Chem. Soc.* **1985**, *107*, 3800–3810.

(80) Dewar, M. J. S. *J. Am. Chem. Soc.* **1984**, *106*, 669–682.

(81) Cremer, D. *Tetrahedron* **1988**, *44*, 7427–7454.

(82) Smith, M. B.; March, J. *Advanced Organic Chemistry: Reactions, Mechanisms, and Structure*, 5th ed.; Wiley: New York, 2001.